ISSN: 0973-3469, Vol.23, No.(1) 2026, Pg. 59-70

Material Science Research India

www.materialsciencejournal.org

Experimental Design Approach to Optimize HA/β-TCP Nanocomposite Formation by Solution Combustion Process

SAMIR KUMAR GHOSH*[1] and SANKAR NARAYAN PATRA[2]

[1]Department of Biomedical Engineering, Netaji Subhash Engineering College, Kolkata, India
[2]Department of Instrumentation and Electronics Engineering, Jadavpur University, Kolkata, India

Abstract

Nano hydroxyapatite and β tricalcium phosphate (HA/β-TCP) composite materials with predesigned phase composition were successfully synthesized via solution combustion route using calcium nitrate tetrahydrate, diammonium hydrogen phosphate and glycine as the fuel. The investigations revealed that combustion flame temperature and its duration depend on several process parameters, and both play a key role in finding out the characteristics of the synthesized powders. An optimal parametric setting was established using Taguchi's design of experiments (DoE) technique to control flame temperature in terms of achieving the best product characteristics. It was found that the optimal parametric combination, consisting of batch size of 6 g, total valence of reducing and oxidizing agent (fuel to oxidizer) ratio of 0.8 and starting furnace temperature of 500 °C, resulted nano sized HAp/β-TCP) composite powders with particle sizes less than 100 nm.

Article History
Received: 19 January 2026
Accepted: 17 March 2026

Keywords
ANOVA;
Combustion Synthesis;
HA/β-TCP Composite;
Nanoparticle;
Optimization of Reaction Parameters
Signal to Noise Ratio.

Introduction

Calcium phosphates bio-ceramics are widely used as bone substitutes due to close mineralogical similarity to biological bones. These materials offer several additional advantages, like highly biocompatible, nontoxic and exhibit bioactive behavior. Many researchers[1-2] have reported that though calcium hydroxyapatite (HA) is highly biocompatible and good osteoconductive, it suffers from limited bioactivity due to its poor stability and hence extremely slower rate of degradation in biological fluids. This limitation is often overcome using bi phasic calcium phosphate (BCP) which combines the long-term stability of HA with the superior bioactivity and higher solubility of beta tricalcium phosphate (β-TCP).[2] The phase ratio can be tailored for specific degradation needs; however, ~40% HA and 60% β-TCP is widely regarded as optimal for bone tissue engineering, especially as a bone graft extender.[1] Preparation of single-phase

CONTACT Samir Kumar Ghosh samirk.ghosh@nsec.ac.in Department of Biomedical Engineering, Netaji Subhash Engineering College, Kolkata, India

© 2026 The Author(s). Published by Enviro Research Publishers.
This is an Open Access article licensed under a Creative Commons license: Attribution 4.0 International (CC-BY).
Doi: http://dx.doi.org/10.13005/msri/230106

calcium hydroxyapatite (HA) and phase designed HA/β-TCP composite with desired properties for biomedical applications remains a great challenge for researchers. Physical and chemical properties of fabricated sample are strongly governed by the properties of starting powders, such as particle size and distribution, phase composition and phase stability. In recent years, several researchers[3-6] have attempted to optimize the powder properties by using various processes. Many routes for synthesizing calcium phosphate powders have been developed to control the powder properties, namely solid state,[7]wet chemical precipitation,[8-10] sol-gel,[11-15] hydrothermal,[16-20] mechanochemical,[21] etc.

However, in many of these approaches, precise control over initial parameters—such as the calcium-to-phosphorus atomic ratio (Ca/P), pH values above 9—and final product characteristics, including phase composition, phase stability, and particle size, remains difficult to achieve.

Nowadays solution combustion method is widely employed for synthesizing ultrafine oxide ceramic powders.[22-29] The technique is particularly effective in controlling the process parameters[29] which have a strong effect on the physiochemical properties of synthesized powder. The solution combustion[22-29] involves an exothermic self-propagating chemical reaction between a metal oxidant and a water-soluble carbonaceous fuel, (commonly citrate, glycine and urea etc.) in an aqueous medium. Solution combustion reaction process is started at relatively lower temperature regime (viz., ~ 400^{o}C), followed by sudden temperature rise subsequent rapid cooling ensures nucleation of maximum number of crystallites but restricts particle growth due to formation of large volume of gases molecules. Consequently, the as-synthesized material consists of voluminous, soft, porous mass that can easily be converted into nano grade powders. Principal advantages of the process include the ability to synthesize predesigned composition with high grades of purity, excellent homogeneity with nano sized powders in one step. Additionally, formation of huge volumes of gases molecules during the exothermic reaction further prevents the particles overgrowth.

In this solution combustion process, calculation of exact amount of reducing to oxidizing mixture is crucial. Based on propellent chemistry, Jain *et al*[30] established a technique to evaluate the degree of oxidizing and reducing power of the combustion process. The system released maximum heat energy when the reducing and oxidizing balance is in stoichiometric (μ=1). The stoichiometric composition of solution combustion is determined by considering the valences of all oxidizing and reducing elements of the reactants and their value is unity. The solution combustion produced an incandescent flame and the highest temperature attained is called to as the 'flame temperature (Tc) which has a significant influence on product properties, such as phase composition, particle size and specific surface area etc. The maximum flame temperature and its duration are strongly correlated with various process parameters, including the type of fuel, reducing to oxidizing ratio (μ), yield and the starting reaction temperature (T), all of which collectively govern the flame temperature and the properties of the synthesized powders.[31–33] Previous studies indicate that stable phase occurs when the combustion flame temperature isaround 780–800°C.[27–28] Based on this studies, 800°C was chosen as a target flame temperature in the present study.

Materials & Methods

The selection of a design of experiment (DoE) depends on the final focus of the investigation and the number of important parameters to be checked. The focus of this investigation was: (i) to optimize parametric set up level of the solution combustion process parameters and to find out the degree of influence of individual parameter on the process outcomes, (ii) to predict the cause–effect relationship between the true system response and the input reaction parameters. To achieve these objectives, Taguchi's technique34 was employed in this investigation. Taguchi's Design of Experiments (DoE) approach was applied to overcome optimization challenges and systematically evaluate the influence of individual process parameters on the response. This technique has been extensively applied across various fields of engineering and science for process optimization and for assessing the effects of multiple design parameters within a given parameter combination. Accordingly, the integration of experimental design and parametric optimization of solution combustion was achieved using the Taguchi approach. In this present work, the desired response was defined as

achieving a target flam temperature in the solution combustion process.

In the present work, the experiments were designed and conducted using Taguchi's orthogonal array methodology.[29, 34] The Taguchi orthogonal arrays are particularly effective in exploring the whole variables space with a relatively smaller number of experimental runs. This technique facilitates the study of the influence of process control variables and noise elements enables the identification of optimal properties for specific uses.

Based on preliminary experimental observations, the most crucial process control factors and their respective levels were identified as yield amount, B, fuel to oxidizer ratio,μ, initial reaction temperature, T Experimental results showed that the yield batch size (B) ranged from 4 to 10, the fuel-to-oxidizer ratio (μ) from 0.8 to 2.8, and the initial furnace temperature (T) was set at 400°C.

Taguchi orthogonal arrays are fractional factorial experimental designs in which the columns are balanced and mutually orthogonal, ensuring that all factor-level combinations occur an equal number of times. This unique feature allows the influence of individual factors on the reaction outcomes to be estimated separately from the other reaction factors. The present study, an L16 Taguchi orthogonal array was used, consisting of three system variables at four levels of individual. The process parameters, their corresponding levels, and the experimental design matrix (in coded form) are presented in the following table1&2 respectively

Table 1: Solution combustion process parameters with their levels

			Taguchi			
Sl No	**Parameter**	**Notation**	**Level1**	**Level2**	**Level3**	**Level4**
1	Batch size (g)	'B'	4	6	8	10
2	Reducing to oxidizing ratio	'μ'	00.8	1.00	1.80	2.80
3	Starting furnace temperature (^{0}C)	'F'	400	500	600	700

Table 2: Taguchi L16 design matrix, responses (Tc) and Signal to noise ratio

SL NO	**B**	**μ**	**F**	**Measured flame temperature (T_c)**	**S/N ratio (dB)**	**Flame duration (sec)**
1	1	1	1	712	21.69	12
2	1	2	2	792	42.97	16
3	1	3	3	788	39.42	19
4	1	4	4	778	34.10	20
5	**2**	**1**	**2**	**802**	**55.06**	**14**
6	2	2	1	850	27.36	18
7	2	3	4	873	24.19	22
8	2	4	3	819	35.60	26
9	3	1	3	862	25.55	19
10	3	2	4	885	22.93	28
11	3	3	1	862	25.55	31
12	3	4	2	826	32.91	24
13	4	1	4	832	31.14	21
14	4	2	3	893	22.19	38
15	4	3	2	878	23.64	39
16	4	4	1	762	29.27	23

Hydrated calcium nitrate and diammonium hydrogen phosphate were used as starting raw materials for the preparation of the target composite. Analytical-reagent-grade glycine was employed as the fuel for the combustion reaction. For the synthesis of the target composite, predetermined aqueous solutions of metal nitrate, AR grade and diammonium hydrogen phosphate (DAP), $(NH_4)_2HPO_4$ (A.R. grade), were slowly mixed under continuous magnetic stirring at room temperature. The calcium-to-phosphorus atomic ratio was strictly maintained at 1.5520 and 1.5690. The initially formed white precipitate was subsequently dissolved by adding 3ml of concentrated nitric acid. Thereafter, required quantity of glycine was mixed to the solution and make a clear homogeneous solution with the help of magnetic stirrer at room temperature.

Then the precursor prepared was transferred to a reaction container of ceramic-coated mild steel container and placed into a kanthal wire muffle furnace at 300–700°C. The reaction container was covered by a wire mesh to minimize particle loss due to aerosol formation. With the help of "K-type" thermocouple, complete temperature–time phenomena were captured of the combustion reaction. At initial stage, the precursor solution boiled vigorously with the evolution of large volumes of gases. The viscous precursor then frothed, followed by the sudden emergence of an incandescent flame. The heat generated during the exothermic reaction was self-sustaining and completed without the need for external energy supply. The steps of the process are represented in Figure I.

A Z-trend paperless chart recorder recorded the time temperature profile of the reaction. (USA made, Honeywell,) Philips, XRD (Cu–Kα_1 radiation, λ = 0.154056 nm, a Ni filter). From the XRD spectrum, average crystallite size of the product was calculated by using the line-broadening method based on the Scherrer equation:

$$D = \frac{0.9\lambda}{\beta \cos\theta}$$

where D, average crystallite size in nm, λ wavelength of the X-ray radiation, θ, the Bragg angle, and β, the full width at half maximum (FWHM) of the most intense diffraction peak corresponding to the (210) plane of β-TCP.

The powder morphology and particle size, shape, and surface area of the synthesized powders were investigated using a scanning electron microscope (SEM) (Leo 430i, U.K.). Prior to SEM analysis, the powders were gently crushed and ultrasonicated in laboratory-grade isopropanol for approximately 5 minutes. The well-dispersed powders thus obtained were used for the morphological investigations.

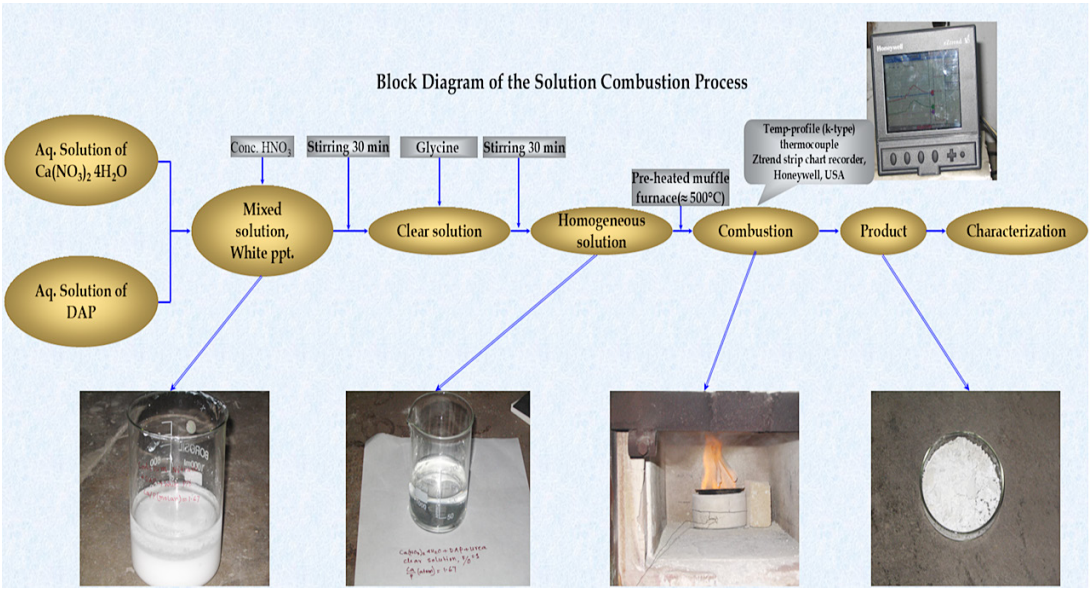

Fig. 1: Block diagram of Solution Combustion Synthesis method

Results & Discussion

Influence of Reaction Parameters on Combustion Flame

Data Analysis and Determine Optimum Parametric Levels using Signal to Noise Ratio

To corelate the effects of individual process parameters on the process outcomes (flame temperature, Tc) and to determine the best parametric combination, Taguchi's DoE performance determine known as the signal to noise ratio was employed. In this Taguchi approach, the Signal to noise ratio is used to identify restrict factor values that are least sensitive to noise factors. The signal indicates the mean response value, while the noise shows the variability around the mean, thereby indicating the sensitivity of the experimental output to uncontrollable factors. The selection of an appropriate S/N ratio be determined by on the quality characteristic of the outcome or system to be optimized.[34]

In Taguchi method used 3 types of signals to noise ratios: "nominal is best" (NB), "lower the better" (LB), and "higher the better" (HB). The appropriate selection criterion chosen is based on previous experience and identifying of the system. In the present investigation, the quality feature of the solution combustion reaction was selected as the reaction maximum temperature. Optimal results are obtained when the response is close to a target value, since stable phase formation of biphasic composite powders with nanoscale features occurs when the flame temperature lies in the range of 780–800 °C.[27–28] Accordingly, a target flame temperature (Tc) of 800 °C was selected, and the nominal-is-best (NB) criterion was adopted for optimization in this study.

Signal to noise ratio for the NB type was calculated using the following expression:

$$S/N = 10\,log_{10}\left(\frac{y^2_{avg\,(i)}}{\sigma_i^2}\right)$$

here, $y_{avg(i)}$: average of i^{th} experimental output and target value; σ_i standard deviation of i^{th} outcomes.

Analysis of Sgnal to Noise Ratio(S/N)

Based on the results summarized in Table II (L16), the signal to noise ratios corresponding to the recorded flame temperature for individual run were determined and are also presented in Table II. In Taguchi's designs, the effects of individual process parameters at different levels can be readily isolated and analysed. In the present S/N ratio analysis, the mean S/N ratio for the batch size at all Levels (i.e.1,2,3&4) was obtained by taking the average of all S/N ratios of experimental Runs in the 1 to 4, 5 to 8, 9 to 12 and 13 to 16 respectively. The same methodology was used to evaluate the mean signal to noise ratios at all levels of the remaining process parameters.

Figure II illustrates the S/N response plot for the maximum temperature, while the main effects plot showing the direct influence of reaction variables on the outcome is shown in Figure III. The mean responses for each process parameter at different levels are listed in Table III.

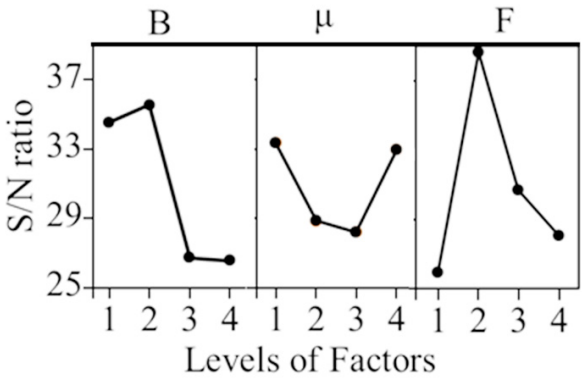

Fig. 2: Main effects plot showing the effect of process parameters on the S/N ratio of the measured flame temperature (Tc)

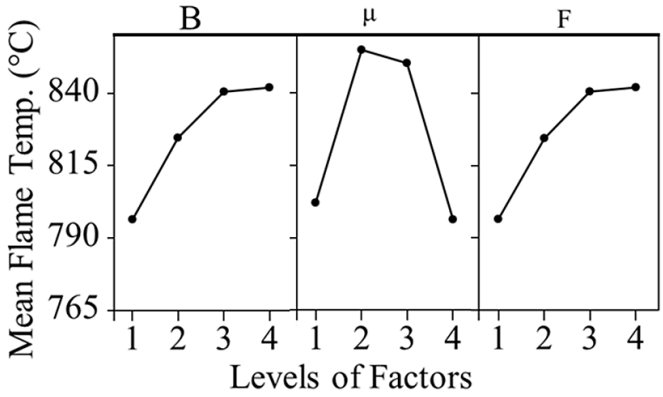

Fig. 3: Influence of process parameters on the flame temperature

Table 3: Mean responses of the process parameters at various levels

"Variable"	"Level:1"	"Level :2"	"Level: 3"	"Level: 4"	"Rank"
B	767.5	836	858.75	841.25	1
μ	802	855	850.25	796.25	2
T	796.5	824.5	840.5	842	3

A higher signal-to-noise (S/N) ratio indicates improve quality performance, regardless of the selected quality characteristic. Accordingly, the optimal process parameter levels are those that yield the highest S/N ratio.. From the S/N ratio analysis shown in Fig. II, the optimal parametric combination for the desired flame temperature is B2.μ1.F2

corresponding to level 2 of batch size (B), level 1 of fuel-to-oxidizer ratio (μ), and level 2 of starting furnace temperature (T).

Based on the S/N ratio analysis shown in Fig. 2, the optimal parametric combination for achieving the target flame temperature is, corresponding to level 2 of batch size (B), level 1 of fuel-to-oxidizer ratio (μ), and level 2 of initial furnace temperature (T).

Furthermore, the mean response values presented in Table III and the main effects plot shown in Fig. III clearly indicate that batch size (B) is the most influential factor affecting the combustion flame temperature, followed by the fuel to oxidizer ratio (μ) and the starting furnace temperature (T). Yield size (B) and staring furnace temperature exhibit a positive influence on the flame temperature, whereas the fuel-to-oxidizer ratio shows an initial increasing effect followed by a declining curve.

Analysis of Variance: ANOVA

The main purpose of analysis of variance or ANOVA is to find the system variables that extensively influence the quality characteristics. Additionally, F-test is also performed to determine the statistical significance of each process parameter on the reaction combustion flame temperature. ANOVA results are presented in Table IV.

The percentage contribution of variance (P) is given by:

$$P = \frac{SS'}{ST}$$

Here, SS': pure sum of square; ST : total sum of square. F-ratio of a parameter is the ratio of variance of that parameter and variance of error.

From Table IV, the ANOVA results clearly indicate that batch size is the most significant parameter influencing the reaction combustion flame temperature, with a percentage contribution of 43.47%. This observation is consistent with the

mean response analysis of the process parameters presented in Table III. The fuel-to-oxidizer ratio is the second most influential factor, contributing 23.45% to the total variance. In contrast, the initial furnace temperature shows the least influence, with a contribution of 7.42%.

Table 4: ANOVA results for recorded flame temperature

"Source"	"DF"	"Sum of Square"(SS)	"Mean Square" (MS)	"F-Value"	"Pure sum of square" (SS')	"Percentage influence" (P)
B	3	19309	6436.4	15.55	16825	43.47
μ	3	11560	3853.4	9.31	9076	23.45
T	3	5355	1784.9	4.31	2871	7.42
Error	6	2484	413.9			
Total	15	38708				

Product Characterization

Additionally, the effect of flame duration (s) on the characteristics of the synthesized powders was investigated. Figure IV(a) presents the time–temperature profiles obtained from the experiments, which indicate that both the flame temperature and flame duration increase with increasing batch size. A larger reactant mass in the solution combustion reaction releases greater enthalpy, leading to a higher flame temperature and longer combustion duration. Figure IV(b) shows that the flame temperature reaches its maximum at the stoichiometric fuel-to-oxidizer ratio, whereas in both fuel lean and fuel rich combustion reaction produce comparatively lower combustion temperatures. At the stoichiometric ratio, the combustion reaction proceeds to completion, leading to the highest flame temperature. In contrast, a fuel-lean system results in incomplete combustion and hence lower flame temperatures. On the other hand, in a fuel-rich system, additional oxygen from the surrounding air is required to complete the combustion of excess fuel. Therefore, the flame temperature decreases, but the combustion duration becomes longer.

Figure IV(c) illustrates the effect of initial furnace temperature on reaction flame temperature and flame duration. An increase in furnace temperature leads to an increase in flame duration; however, no significant change in flame temperature is observed. The probable reason for the extended combustion duration at higher initial furnace temperatures is the reduced rate of heat loss to the surroundings.

XRD analysis of the synthesized powders revealed that longer flame duration adversely affects crystallite size, promoting increased crystallite growth.

Figure V shows the X-ray diffraction patterns of selected as processed powders obtained by the solution combustion reaction using a calcium metal nitrate, DAP and glycine system at B2·μ1·F2, corresponding to levels 2, 1, and 2 of yield size (B), fuel to oxidizer ratio (μ), and starting furnace temperature (T), respectively. To tailor the phase composition of the as-synthesized powders, two different calcium-to-phosphorous (Ca/P) ratios, namely 1.5520 and 1.5690, were employed in this work.

The crystalline phases were identified using JCPDS file No. 09-0432 (HAp) and No. 09-0169 (β-TCP). The XRD patterns show well-defined crystalline phases of HAp and β-TCP in the synthesized powders. The percentage of volume of each phase was estimated from the powder XRD patterns by comparing the integrated intensities of the characteristic peaks of each phase, as the integrated intensity is proportional to the corresponding volume fraction. The volume fraction was calculated using the following relation:

$$\beta - TCP = \frac{I_{\beta-TCP}}{I_{\beta-TCP} + I_{HA}}$$

Here $I_{\beta\text{-TCP}}$ and I_{HA} are the integrated values of peak intensities of β-TCP and HAp phases, respectively. The calculated volume fractions of β-TCP and

HAp were approximately 70.12% and 29.88%, respectively, for a Ca/P ratio of 1.5520 in the precursor batch. For a Ca/P ratio of 1.5690, the corresponding volume fractions of β-TCP and HAp were found to be 60.48% and 39.52%, respectively.

The results clearly indicate that the Ca to P atomic ratio significantly influences the phase composition of the synthesized powders.. The chemical analysis of both as-synthesized powders is presented in Table V.

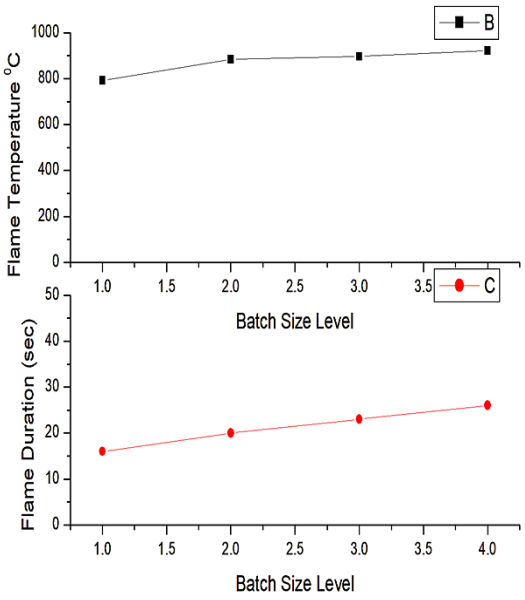

(a) B vs combustion flame duration (t) and T_c

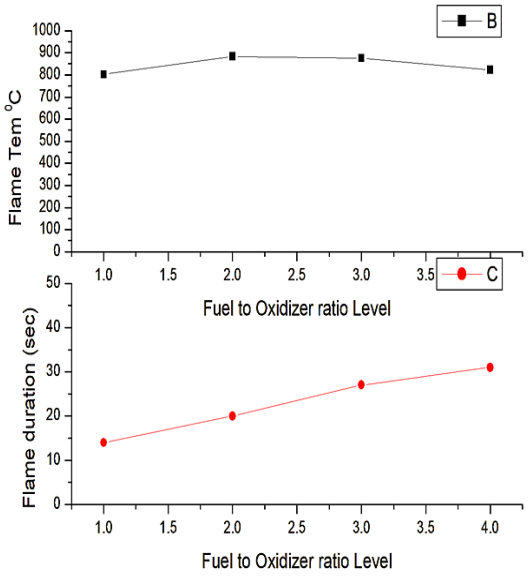

(b) μ vs combustion flame duration (t) and T_c

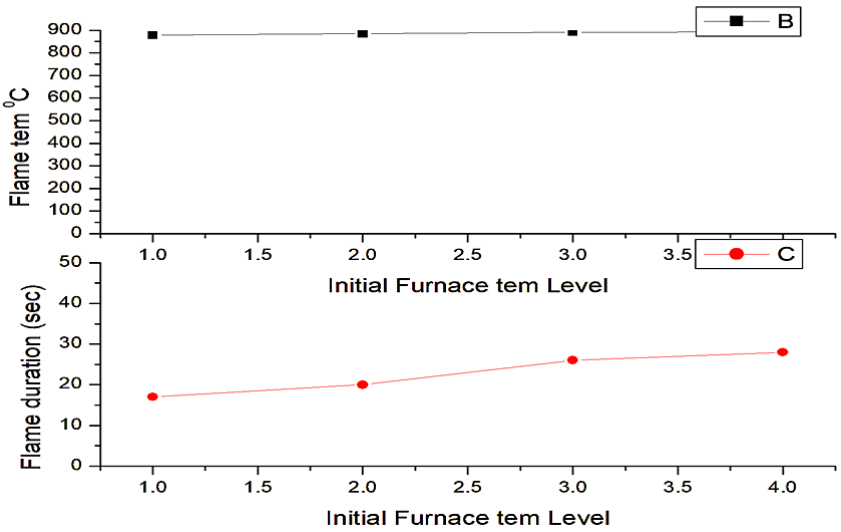

(c) T vs combustion flame duration (t) and T_c

Fig.4: (a) B vs combustion flame duration (t) and T_c;(b) μ vs combustion flame duration (t) and T_c; (c) T vs combustion flame duration (t) and T_c

Furthermore, the temperature above 800 °C were necessary to obtain well-crystallized composite powders.. Powders synthesized below 800 °C were amorphous or poorly crystalline and required post-heat treatment to obtain well-crystallized biphasic calcium phosphate (BCP) powders.. The crystallite size, calculated from XRD analysis, increased with increasing flame temperature and flame duration. Higher flame temperatures combined with longer combustion durations promote a sintering effect, leading to crystallite growth. This trend is further corroborated by the average particle size measurements obtained from SEM analysis, as shown in Figure VI.

Many researchers[35-36] have employed X-ray diffraction (XRD), scanning electron microscopy (SEM), and field emission scanning electron microscopy (FESEM) techniques to confirm the nanostructured nature of synthesized materials in their studies. In the present investigation, SEM micrographs of the synthesized powders revealed the formation of fine agglomerated particles with nanoscale dimensions. The individual particles appear nearly spherical and are uniformly distributed, indicating the successful synthesis of nanoparticles. The particles also exhibit a highly porous and agglomerated morphology, which is commonly observed in powders produced by the solution combustion synthesis method due to the rapid evolution of gases during the combustion process. The observed morphology therefore confirms the formation of nanostructured materials. Furthermore, the XRD pattern exhibited characteristic diffraction peaks corresponding to the crystalline phase of the synthesized material. The diffraction peaks were noticeably broadened, which is a typical indication of the nanocrystalline nature of the powder. The average crystallite size was estimated using the Scherrer equation and was found to be in the nanometre range. These results further confirm the successful formation of nanoparticles.

Table 5: Chemical analysis of precursor solution and as synthesized BCP powders

Ca/P atomic ratio in precursor sample	Chemical analysis of as synthesized		
	%wt. Ca	%wt. P	Ca/P atomic ratio
1.5520	36.3640	18.185	1.5498
1.5690	35.6878	17.700	1.5632

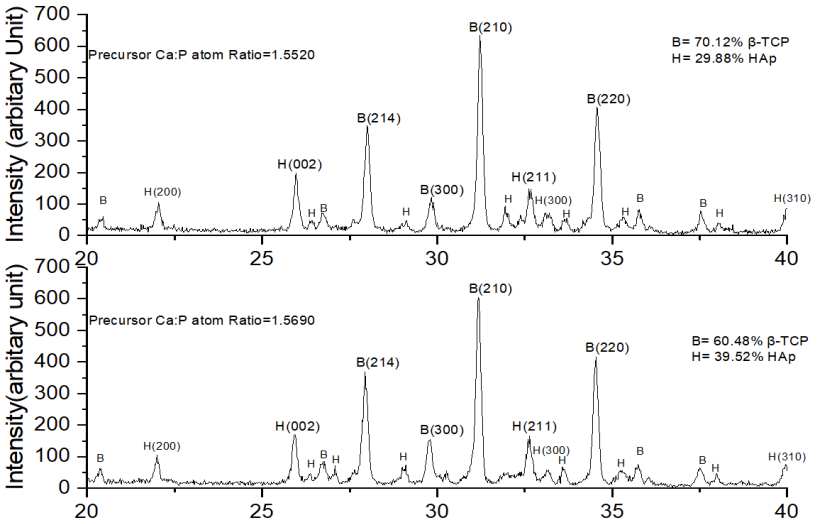

Fig. 5: shows the XRD pattern of as synthesized powders of optimal parametric combination (B2.μ1.F2) (a) Ca to P atom =1.5520 and (b) Ca to P atom=1.5690

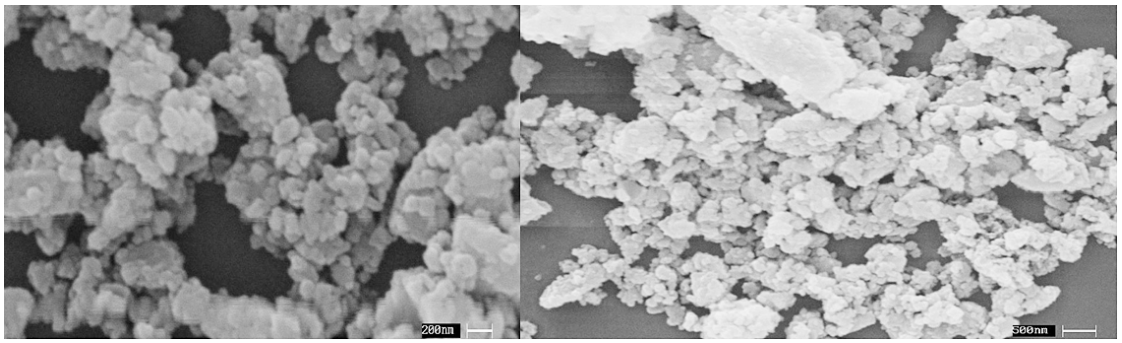

Fig. 6: shows the SEM pattern of as synthesized powders of optimal parametric combination (B2.μ1.F2) (a) Ca/P=1.5520 and (b) Ca/P=1.5690

Conclusion

In this study, Taguchi DoE technique was successfully applied to optimize the solution combustion synthesis of nanostructured, predesigned HA/β-TCP composite powders. The optimal combination of solution combustion process parameters for obtaining powders with 60.48% β-TCP and 39.52% HA was identified as B2·μ1·F2, corresponding to levels 2, 1, and 2 of yield size (B), fuel to oxidizer ratio (μ), and starting reaction temperature (T), separately. Under these optimized conditions, a flame temperature of 802 °C, a flame duration of 14 s, an average particle size of 86 nm, and a crystallite size of 38 nm were achieved.

The signal to noise ratio analysis and ANOVA identified batch size (B) as the most influential parameter, followed by the fuel to oxidizer ratio (μ). In contrast, the starting furnace temperature (T) was found to have no significant effect on the maximum combustion flame temperature because maximum heat is generated from the reaction mass and its enthalpy An increase in batch size and initial furnace temperature prolonged the flame duration, leading to enhanced particle growth and crystallite coarsening in the as-synthesized powders.Conversely, an increase in the fuel-to-oxidizer ratio promoted the formation of finer particles with reduced crystallite sizes.

Overall, the Taguchi DoE–based optimized parameters enabled the successful synthesis of nanocomposite of HA/β-TCP powders with controlled phase composition and desirable microstructural features, demonstrating the effectiveness of this approach for solution combustion synthesis.

Acknowledgement

The research work is supported by Netaji Subhash Engineering College, Techno India, WB, India and Department of Electronics and Applied Instrumentation, Jadavpur University, Kolkata, India. The authors wish to thank Prof. Sukhomay Pal, Mechanical Engineering, IIT Guwahati, India for his continuous encouragement in this regard.

Funding Sources

The author(s) received no financial support for the research, authorship, and/or publication of this article

Conflict of Interest

The authors do not have any conflict of interest.

Data Availability Statement

This statement does not apply to this article.

Ethics Statement

This research did not involve human participants, animal subjects, or any material that requires ethical approval.

Permission to reproduce material from other sources

Not applicable.

Author Contributions

- **Samir Kumar Ghosh(S.K.G):** Experimental and Analysis, Making Methodology and Data Analysis.
- **Sankar Narayan Patra:** Implementation of DoE and Analysis and Writing the Parametric Optimization Process.

References

1. Lee, J.H., Ryu, M.Y., B., H.R., Lee, K.M., Seo, J.H. and Lee, H.K., Fabrication and evaluation of porous beta-tricalcium phosphate/hydroxyapatite (60/40) composite as a bone graft extender using rat calvarial bone defect model, *The Scientific World Journal*, 2013;16: Article ID 481789, 8 pages
2. Daculsi, G., Biphasic calcium phosphate concept applied to artificial bone, implant coating and injectable bone substitute, *Biomaterials,* 1998;19 (16):1473–1478.
3. Best, S. and Bonfield, W., Composition of hydroxyapatite and its relationship to the electrical properties of bone, *J. Mater. Sci.: Mater. Med.*1994; 5 (6): 516–522.
4. Le Geros, R.Z., Properties of osteoconductive biomaterials: calcium phosphates, *Clin. Orthop. Relat. Res.,* 2002;395: 81–98.
5. Stupp, S.I. and Ciegler, G.W., Synthesis of nanophase hydroxyapatite/collagen composite, *J. Biomed. Mater. Res.*1992; 26 (2):169–183.
6. Osaka, A., Miura, Y., Takeuchi, K., Asada, M. and Takahashi, K., Development of calcium phosphate-based apatite from hen's eggshell, *J. Mater. Sci.: Mater. Med.*1991; 2 (1):51–55.
7. Otsuka, M., Matsuda, Y., Hsu, J., Fox, J.L. and Higuchi, W.I., Mechanochemical synthesis of bioactive material: Effect of environmental conditions on the phase transformation of calcium phosphates during grinding, *Bio-Med. Mater. Eng.*1994; 4 (5):357–372.
8. Bernard, L., Freche, M., Lacout, J.L. and Biscans, B., Preparation of hydroxyapatite by neutralization at low temperature: influence of purity of the raw material, *Powder Technol.*1999;103 (1):19–25.
9. Mavis, B. and Tas, A.C., Dip coating of calcium hydroxyapatite on Ti–6Al–4V substrates, *J. Am. Ceram. Soc.*2000;83 (4):989–992.
10. Aoki, H. and Kato, K., Biphasic calcium phosphate bioceramics: preparation, properties and applications, Ceram. *Jpn.*1975;10 (6):469–474.
11. Cheng, K., Shen, G., Weng, W., Han, G., Ferreira, J.M.F. and Yang, J., Synthesis of hydroxyapatite/fluoroapatite solid solution by a sol–gel method, *Mater. Lett.*, 2001;51 (1): 37–41.
12. Feng, W., Mu-sen, L., Yu-peng, L. and Yong-xin, Q., A simple sol–gel technique for preparing hydroxyapatite nanopowders, *Mater. Lett.*, 2005;59 (7):916–919.
13. Weng, W.J. and Baptista, J.L., The facile and low temperature synthesis of nanophase hydroxyapatite crystals using wet chemistry, *Biomaterials,* 1998;19 (1–3): 125–131.
14. Liu, D.-M., Troczynski, T. and Seng, W.J.T., Water-based sol–gel synthesis of hydroxyapatite: process development, *Biomaterials*, 2001;22 (13):1721–1730.
15. Liu, D.-M., Yang, Q., Troczynski, T. and Tseng, W.J., Structural evolution of sol–gel-derived hydroxyapatite, *Biomaterials*, 2002;23 (7):1679–1687.
16. Zhang, S. and Consalves, K.E., Microemulsion-mediated synthesis of calcium hydroxyapatite fine powders, *J. Mater. Sci.: Mater. Med*. 1997;8 (1): 25–28.
17. Liu, H.S., Chin, T.S., Lai, L.S., Chiu, S.Y., Chung, K.H., Chang, C.S. and Liu, M.T., Hydroxyapatite synthesized by a simplified hydrothermal method, Ceram. *Int.*1997;23 (1):19–25.
18. Suchanek, W. and Yoshimura, M., Preparation of fibrous, porous hydroxyapatite ceramics from hydroxyapatite whiskers, *J. Am. Ceram. Soc.*1998; 81 (3):765–772.
19. Lim, G.K., Wang, J., Ng, S.C. and Gan, L.M., Processing of hydroxyapatite via microemulsion and emulsion routes, *Biomaterials*, 1997;18 (21):1433–1439.
20. Yoshimura, M., Suda, H., Okamoto, K. and Ioku, K., Hydrothermal synthesis of biocompatible whiskers*, J. Mater. Sci.*1994;29 (13):3399–3402.
21. Gutman, E., Mechanochemistry of materials: The fundamental principles of mechanically induced chemical reactions in solids, Cambridge International Science Publishing, UK, 1997.
22. Kingsley, J.J. and Patil, K.C., A novel combustion process for the synthesis of fine particle α-alumina and related oxide materials, *Mater. Lett.*1988; 6(11-12):427-432, 1988.

23. Kingsley, J.J., Suresh, K. and Patil, K.C., Combustion synthesis of fine-particle metal aluminates, *J. Mater. Sci*.1990; 25(3):1305-1312.
24. Manoharan, S.S. and Patil, K.C., Combustion synthesis of metal chromite powders, *J. Am. Ceram. Soc.*1992;75:1012-1015.
25. Zhang, Y. and Stangle, G.C., Preparation of fine multicomponent oxide ceramic powder by a combustion synthesis process, *J. Mater. Res.*1994; 9: 1997-2004.
26. Segadges, A.M., Morelli, M.R. and Kiminami, R.G.A., Effect of fuel type on morphology and reactivity of combustion synthesized alumina, *J. Eur. Ceram. Soc*.1998; 18: 771.
27. Ghosh, S.K., Pal, S., Roy, S.K., Pal, S.K. and Basu, D., Synthesis of nano-sized hydroxyapatite powders through solution combustion route under different reaction conditions, *Mater. Sci. Eng. B*,2011:176:14–21, .
28. Ghosh, S.K., Datta, S. and Roy, S.K., Solution combustion synthesis of calcium hydroxyapatite nanoparticles, Trans. *Indian Ceram. Soc.*2004;63: 27.
29. Ghosh, S.K., Pal, S., Roy, S., Pal, S.K. and Basu, D., Modelling of flame temperature of solution combustion synthesis of nanocrystalline hydroxyapatite material and its parametric optimization, *Bull. Mater. Sci.,* 2010;33 (4):339-350.
30. Jain, S.R., Adiga, K.C. and Pai Vernekar, V.R., A new approach to thermochemical calculations of condensed fuel–oxidizer mixtures, Combust. *Flame,* 1980;40:71.
31. Ghosh, S.K., Nandi, S.K., Kundu, B., Datta, S., De, D.K., Roy, S.K. and Basu, D., In vivo response of porous hydroxyapatite and beta-tricalcium phosphate prepared by aqueous solution combustion method and comparison with bioglass scaffolds, *J. Biomed. Mater. Res. B Appl. Biomater*., 2008;86:217–227.
32. Yuan, Y., Liu, C., Zhang, Y. and Shan, X., Structure and photoluminescence properties of ZnS:Mn nanocrystals synthesized by a simple hydrothermal method, *Mater. Chem. Phys.,* 2008;112:275–280.
33. Purohit, R.D., Saha, S. and Tyagi, A.K., Nanocrystalline thoria powders via glycine-nitrate combustion*, J. Nucl. Mater.*,2001; 288:7–10.
34. Roy, R.K., Design of Experiments Using the Taguchi Approach, John Wiley & Sons Inc., New York, 2001.
35. Priyadarshini, B., *et al*., In situ fabrication of cerium-incorporated hydroxyapatite/ magnetite nanocomposite coatings., *Nanoscale Advances*, 2023;5: 5054–5076.
36. Kawsar, M., Hossain, M. S., Tabassum, S., Islam, D., Bahadur, N. M., & Ahmed, S. (2024). Crystal structure modification of nano-hydroxyapatite using organic modifiers and hydrothermal technique., *RSC Advances,* 2024;14: 29665–29674.